Quantum Electronics **30** (2) 152 – 157 (2000)

INVITED PAPER

PACS numbers: 42.55.Px; 73.20.Dx; 85.30.Vw
DOI: 10.1070/QE2000v030n02ABEH001677

Analysis of absorption and amplification in a unipolar semiconductor structure with quantum dots

P G Eliseev

Abstract. The allowed intraband optical transitions in a quantum dot are considered in the context of their application in quantum-well IR detectors and unipolar semiconductor lasers. The atom-like quantum dot is described by using the harmonic oscillator model. An expression is obtained for the absorption cross section which is independent of the wavelength and the quantum-dot size. Optical absorption and amplification are estimated.

1. Introduction

The unipolar optical transitions (transitions of a carrier of a certain sign between the subbands in a quantum-size structure) have been used successfully in semiconductor optoelectronic devices, such as quantum-cascade lasers (QCLs) [1] and quantum-well IR photodetectors (QWIPs) [2, 3]. Along with the 2-D electron gas structures, new structures containing the so-called quantum dots can be used for the same purpose, which offer some advantages [4 – 6]. Quantum dots (boxes) exhibit a discrete energy spectrum, and the selection rules for optical transitions in them may be modified depending on the profile of the potential that provides the 3-D localisation of electrons.

The quantum-dot structures represent a new interesting medium containing artificial atom-like objects ('quasi-atoms'). Unlike the real atoms, a profile of the potential energy in a quantum dot can be optimised for a specific technical problem. First of all, this concerns the choice of a proper spectral range.

In addition, a proper choice of a profile of the potential energy, including the dot geometry, allows one to optimise in principle the selection rules in order to obtain, for example, a required anisotropy or isotropy of the optical interaction. For example, because all the emission outside a single mode in a laser is isotropic and is therefore lost, the isotropy of radiative processes is undesirable.

In real atoms, a significant anisotropy is caused by the stimulated emission, whereas the spontaneous emission remains isotropic. The oriented anisotropic quantum dots, as emitting components of the laser medium would have advantages over real atoms.

P G Eliseev P N Lebedev Physics institute, Russian Academy of Sciences, Leninsky prosp., 53 117924 Moscow (current adress: University of New Mexico, Albuquerque, New Mexico; e-mail eliseev@chtm.unm.edu)

Received 21 May 1999
Kvantovaya Elektronika **30** (2) 152 – 157 (2000)
Translated by P G Eliseev, edited by M N Sapozhnikov

As regards practical implementation of quantum-dot structures, nanotechology offers a variety of methods of epitaxial crystallisation and photolithography for the 3-D confinement of carriers inside a quantum-size object (the typical radius of such an object is 5 – 50 nm). A direct photo-lithographic method allows one to obtain 'quantum discs' with a lateral (largest) size of about 20 – 30 nm. Noticeable progress was achieved in practice by using the technique of a 'self-assembled' growth of quantum dots during the epitaxy of strongly lattice-mismatched materials [4 – 6]. For example, when a small amount of InAs is grown on GaAs, most of the deposited InAs is located in islands with a vertical size of a few nanometres and a lateral size of 20 – 100 nm. Such objects can be also treated as quantum discs or 'quantum pyramids' (because their boundaries resemble crystallographic faces).

Therefore quantum dots with the 3-D confinement of carriers represent real objects in experimental physics. It is likely that quantum-dot lasers on interband (bipolar) transitions will become real devices in the near future. It is interesting that such structures exhibit IR emission, which is related to unipolar transitions in quantum dots [7].

In this paper, the absorption and amplification coefficients of quantum-dot structures are analysed. These quantities play a very important role in the design of real unipolar devices, but they have not been discussed adequately in the literature. In this paper, an expression is obtained for the absorption cross section, which is independent of the wavelength. Because a quantum dot was described by the simplest harmonic oscillator model, the results obtained in the paper can be used only approximately for the description of the structures with another profile. We assume that our qualitative results are quite general.

2. Model of an atom-like quantum dot

The forces acting on an electron or a hole in the region of the chemical gradient are called sometimes 'quasi-electric'. In the band approximation, the chemical composition gradient causes the slope and distortion of the band edges. These deformations can overlap the deformations produced by real electric fields. Therefore, by varying the composition of the structure, one can create the potential wells and barriers that confine the motion of carriers.

To obtain an atom-like object, a 3-D potential well should be created by concentrating the chemical component that provides the narrower band gap. If the components forming the type-I heterojunction are mixed, the well is obtained for carriers of both types. If the components form the type-II heterojunction, the well is obtained for carriers of one type. In the first case, the quantum dot can capture carriers with

opposite signs, remaining neutral (which is equivalent to the exciton capture). In the second case, a carrier of one sign can be readily captured by the dot, whereas to neutralise the bulk, ions or free carriers are required. For example, by increasing the local concentration of InAs in the isovalent GaSb – InAs system, a quantum well can be obtained for electrons, but not for holes. A quantum well for holes can be produced by decreasing the local concentration of InAs.

The energy levels of the quantum dot are determined by the depth and profile of the potential well, as well as by the presence of captured carriers. To simplify the energy spectrum, a doped semiconductor can be considered, which contains, along with quantum dots, comparatively shallow donor centres. In this case, the bulk neutrality is provided by ionised donors, and the electrons are captured at deeper energy levels of quantum dots. If the concentrations of donors and quantum dots are equal, there are no free carriers in the medium. Such a medium is located as a layer between highly doped materials (electrodes) with the conductivity of the same type.

Because a profile of the potential well is determined by the variation of composition of the isovalent components, it can be in principle properly optimised for practical applications. At present, we are able to provide the required spectral range of optical transitions, whereas it is not possible to produce a detailed profile of the potential. The potential profile is smoothed because of some mixing of the components. The final profile can be represented as a well, with smooth edges, for example a parabolic well truncated at the height where the energy reaches the conduction band edge of the surrounding uniform medium (Fig. 1a).

The parabolic potential well for quantum dots or discs was considered, for example, in Ref. [8]. When an electron is strongly localised in such a well, it behaves like a harmonic oscillator. We will use this assumption below. The potential energy profile $U(r)$ in a centrally symmetric well has the form

$$U(r) = \tfrac{1}{2} m^* \omega^2 r^2 \,, \tag{1}$$

where m^* is the effective mass of the carrier (a conduction electron or a hole); ω is the angular frequency of the transition between neighbouring levels. The harmonic oscillator is features equidistant energy levels separated by the distance $\hbar\omega$. The transitions between these levels are working transitions for unipolar optoelectronic devices considered here.

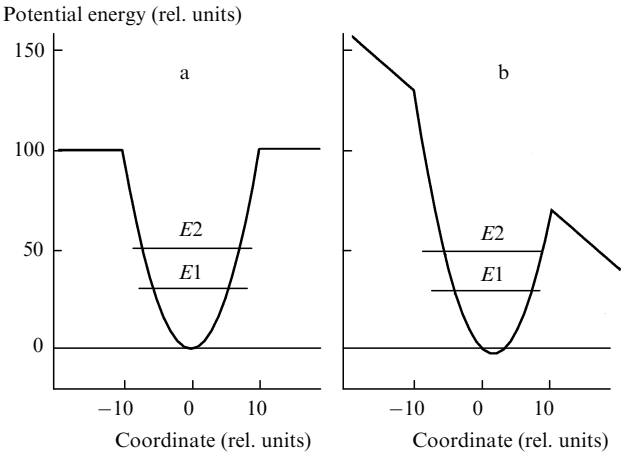

Profile of the potential energy of a quantum dot and positions of the ground ($E1$) and the first excited ($E2$) levels in the absence (a) and in the presence (b) of a uniform electric field. In the latter case, the bottom of the well is displaced but its shape does not change.

3. Unipolar quantum-dot optoelectronic devices

When an external electric field is applied to the quantum-dot structure, the motion of electrons can be accompanied by intracentre transitions. Consider a simple scheme of a photodetector in which a layer (or many layers) of the quantum-dot material is located between unipolar low-resistance 'electrodes'. Although there is an electric field inside the layer, the ground-state electrons are quite strongly coupled with quantum dots and the current is absent in the structure (or is very weak). If upon irradiation by photons the electrons transfer to the excited states (including the resonance states), they may leave the quantum dot, resulting in the appearance of the photocurrent in the structure. It is important to know the value of absorption, which determines the efficiency of a quantum-dot photodetector. Note that such a structure resembles an impurity photoresistor in which quantum dots play the role of impurities. Unlike a chemical impurity, the spectrum of the quantum dot can be 'tailored' in accordance with a specified technical problem.

Because typical energies of the intracentre transitions are usually small compared with the band gap, the above mechanism can be applied first of all to the IR photodetectors. The use of a wide-band-gap system, such as AlN – GaN or GaH – InN allows one to obtain emission not only in the IR but also in the visible region [9].

For a unipolar laser, the pumping mechanism is important. One can imagine a structure that can also be used as a photodetector, where electrons can tunnel resonantly from one electrode to the upper working state of the quantum dot and, similarly, they can tunnel from the ground state to another electrode. This will lead to the population of the upper level and depletion of the lower level, resulting in population inversion.

The use of resonance tunneling in a cascade unipolar laser with a 2-D electron gas was earlier considered in Ref. [10]. The radiative processes inside a quantum dot can be controlled to some degree by a choice of the potential-well profile. The emission wavelength is determined by the energy gap between the working states and can lie in the IR or visible region. In contrast to the structures based on diagonal tunneling, in this unipolar structure the vertical (intracentre) transitions are used.

When an external electric field is applied, the position of the energy levels in the well changes. The effect of a uniform field is shown schematically in Fig. 1b. A minimum of the parabolic well is displaced in the direction of the field by the distance $\Delta x = qF/(m^*\omega^2)$, where q is an elementary charge and F is the electric field strength. The bottom of the well lowers by $\Delta E = -q^2F^2/(2m^*\omega^2)$. However, the shape of the parabola does not change and therefore the position of the local levels relative to the bottom of the well also does not change until the energy barriers become insufficient for electron confinement. Thus, unlike the energy of the interband transition, which exhibits the quadratic red shift, the resonance energy $\hbar\omega$ of the unipolar absorption is in fact insensitive to the electric field until tunnel ionisation begins.

4. Probability of optical transitions

Consider optical transitions between the ground and the first excited state of an electron localised at the quantum dot. The probability of absorption of a photon with the linear polarisation $\boldsymbol{e}_a$ per unit time per solid state element $\mathrm{d}\Omega$ is [11]

$$\mathrm{d}P = \frac{\omega^3 N_{\mathrm{ph}}}{2\pi c^3 \hbar} |\boldsymbol{e}_a \boldsymbol{d}|^2 \, \mathrm{d}\Omega \,, \tag{2}$$

where N_{ph} is the photon density; ω is the angular optical frequency; and $\boldsymbol{d}$ is the transition electric dipole moment. This dipole moment can be calculated, for example, from the expression

$$\boldsymbol{e}\boldsymbol{d}_{ba} \equiv q\langle b|\boldsymbol{e}\boldsymbol{r}|a\rangle \,, \tag{3}$$

where a and b refer to the wave functions of the initial and final states; q is an elementary charge; $\boldsymbol{e}$ is the unit polarisation vector; and $\boldsymbol{r}$ is the radius vector of an electron. The wave functions in the quantum system with a centrally symmetric field can be expressed in terms of the spherical functions $Y_{i,j}(\theta, \phi)$ as

$$|a\rangle = R_a(r) Y_{lama}(\theta, \phi) \,, \quad |b\rangle = R_b(r) Y_{lbmb}(\theta, \phi) \,, \tag{4}$$

where la, ma, lb, and mb are the quantum numbers determining the square of the momentum and its projection to an axis in the initial and final states. When the vector $\boldsymbol{e}$ is directed along this axis, we obtain [11]

$$\boldsymbol{e}\boldsymbol{d}_{ba} = (4\pi/3)^{1/2} \int R_b R_a r^3 \mathrm{d}r \int Y^*_{lbmb} Y_{1,0} Y_{lama} \, \mathrm{d}\Omega \,. \tag{5}$$

An accurate normalisation of the wave functions for oscillators of different dimensionalities is presented in Appendix 1.

5. Dipole moment for the harmonic oscillator

The matrix element for oscillators of different dimensionalities is calculated in Appendix 2. The square of the matrix element $|\boldsymbol{d}^2|$ of the transition between the ground level and the first excited level of the harmonic oscillator is described by the expression

$$|\boldsymbol{d}|^2 = \frac{\hbar q^2}{2m^* \omega} \,, \tag{6}$$

where $\hbar\omega$ is the distance between neighboring levels of the harmonic oscillator (other transitions are forbidden). For example, assuming $m^* = 0.06 m_0$ and $\hbar\omega = 0.13$ eV, we obtain $|\boldsymbol{d}| \sim q \times 1.15$ nm. For comparison, note that the dipole moment for the 0.129 eV intersubband transition (10 μm IR region) in a 2-D electron gas in a rectangular InGsAs quantum well was found to be $q \times (2.34 \pm 0.1\mathrm{nm})$ for a 10 nm thick layer [12]. Note that, because $|\boldsymbol{d}^2|$ increases proportionally to the number of the lower level involved in the transition, the higher the working levels in the energy spectrum of the harmonic oscillator rate, the higher the rate of optical transitions between these levels. The calculation performed for the 2-D well of width L with infinite barriers shows that the dipole moment of transition between the ground and the first excited level is $0.18qL$ [13].

6. Optical absorption in a quantum-dot medium

The absorption coefficient α related to the optical transitions considered above can be calculated from the expression (pp 137 – 139, Ref. [14])

$$\alpha = \frac{(N_0 - N_1)|\boldsymbol{d}|^2 \hbar\omega g(v)}{2\hbar^2 cn\varepsilon_0} \,, \tag{7}$$

where N_0 and N_1 are concentrations of quantum dots in the ground and the first excited state; $g(v)$ is the shape function of the spectral band; ε_0 is the permittivity of vacuum; and n is the refractive index of the medium. It is assumed that the width of the absorption spectrum is determined primarily by a simple Lorentzian broadening. In this case, the absorption coefficient at the band centre is obtained by substituting $g_{\max} = 4\hbar/\Delta E$ instead of $g(v)$, where ΔE is the full width of the shape function of the spectral band at half maximum. In reality, the broadening of the spectrum of quantum dots is caused by the scatter in their size. In this case, the shape of the absorption band is Gaussian, and the absorption coefficient at the center of the band is obtained by the substitution $g_{\max} = 4\hbar(\pi \ln 2)^{1/2}/\Delta E$. The general expression for the maximum absorption at the center of the spectral band has the form

$$\alpha_{\max} = \frac{2\gamma\omega N|d|^2}{\Delta E cn\varepsilon_0} \,, \tag{8}$$

where $\gamma = 1$ for the Lorentzian line shape and $\gamma = 1.476$ for the Gaussian line shape. The effective absorption cross section is defined as $\sigma = \mathrm{d}\alpha/\mathrm{d}N$, where N is the concentration of absorbing centres. Near equilibrium, the relation $N = N_0 \gg N_1$ is valid, and we have

$$\sigma_{\max} = \frac{2\gamma\omega|d|^2}{\Delta E cn\varepsilon_0} = \frac{\gamma q^2 \hbar}{\Delta E m^* cn\varepsilon_0} \,, \tag{9}$$

and in the numerical form (in cm^2),

$$\sigma_{\max} = 7 \times 10^{-17} \frac{\gamma}{n(m^*/m_0)\Delta E} \,, \tag{10}$$

where ΔE is expressed in electron volts. This expression is universal in that it does not depend explicitly on the emission wavelength and the quantum-dot size. The influence of the medium is introduced via the material parameters n, m^*, and ΔE. For $\gamma = 1.476$, $n = 3.3$ and $m^* = 0.06 m_0$ (typical values for the InAs – GaAs structures), $\sigma_{\max}$ lies in the interval from $\sim 5 \times 10^{-14}$ to 5×10^{-15} cm^2, if ΔE changes from 0.01 to 0.1 eV (see table 1).

Let us compare our results with the scarce data on IR absorption that can be attributed to absorption by quantum dots. In Ref. [15], the absorption was observed in the region between 13 and 15 μm for a periodic structure (superlattice) with 20 periods containing quantum dots of InGaAs/GaAs. The microphotographs presented in this paper show that the 2-D density of the quantum dots equals $(5 - 8) \times 10^{10}$ cm^{-2}. The width of the IR absorption band was 11 meV, and absorption was estimated as a few percent for the normal incidence of light. According to our estimate, the absorption cross section is $\sigma = 4.7 \times 10^{-14}$ cm^2, which means that for the bulk density of quantum dots of about $\sim 2.4 \times 10^{16}$ cm^{-3} the expected absorption coefficient is ~ 1130 cm^{-1}. For a structure 680 nm in thickness, the absorbed fraction of the light flux amounts to 7.6%, in satisfactory agreement with the experiment. When absorption is detected by using multipass geometry, the measured absorption becomes greater [15].

The photoinduced absorption by quantum dots in the IR region was observed in Ref. [16]. The structure contained 30 layers with InAs quantum dots separated by the 50 nm thick

Table 1. The absorption cross section and absorption coefficient calculated at the centre of the absorption band for linearly polarised emission in the quantum-dot medium.

ΔE/eV	InAs – GaAs		InGaN – AlN	
	$\sigma/10^{-14}$ cm^2	α/cm^{-1}	$\sigma/10^{-14}$ cm^2	α/cm^{-1}
0.01	5.217	5217	2.174	2175
0.05	1.043	1043	0.4349	435
0.1	0.522	522	0.217	217
0.2	0.261	261	0.109	109

Note: the bulk density of quantum dots is 10^{17} cm^{-3}, $n = 3.3$, $m^* = 0.06m_0$ (for InAs – GaAs), $n = 2.5$, $m^* = 0.19m_0$ (for InGaN – AlN). The result of calculations does not depend on the wavelength at the centre of the absorption band.

GaAs barriers. The 2-D density of quantum dots was 10^{10} to 10^{11} cm^{-2}. The working levels in the undoped structure were populated by illuminating a sample by light at the frequency within the interband absorption band. For this reason, both electrons and holes could both produce absorption bands. However, the relative variation of absorption induced by illumination was about 10^{-4} at wavelength of 6.5 μm. Since the concentration of the populated quantum dots and background absorption are not known, we can say only that the observed effect does not exceed the expected attenuation of the light flux, which is about 1.5% for $N = 2 \times 10^{16}$ cm^{-3}.

To obtain the equilibrium absorption at a level of 1000 cm^{-1}, the bulk concentration of quantum dots should be 2×10^{16} cm^{-3}. The same concentration of shallow donors is required to populate the ground state by electrons. Quantum dots are usually located in the growth plane. For the typical 2-D density $\sim 10^{11}$ cm^{-2} of self-assembled quantum dots of the bulk concentration of $\sim 2 \times 10^{16}$ cm^{-3} is achieved when the distance between the planes is 50 nm. It seems that the production of quantum dots at higher densities will pose significant technological problems. To enhance absorption, the width of the spectrum should be proportionally reduced. This can be achieved by producing quantum dots with a narrower size distribution.

7. Optical amplification in a quantum-dot medium

To calculate the gain, one should know the rates of nonradiative relaxation of the excited state. It is known that the nonradiative lifetime in unipolar lasers on the 2-D electron gas is much shorter than the radiative lifetime. For this reason, the threshold current required to obtain the population inversion is higher than that for usual 'bipolar' lasers. However, the short lifetime of the excited state provides very fast response of unipolar optoelectronic devices (sources, modulators, and photodetectors).

Quantum dots can have advantages over 2-D structures because the nonradiative relaxation in them proceeds slower than in the 2-D structures. To achieve a material gain of 1000 cm^{-1} in the medium described in Section 6, a total population inversion is required.

The case of an incomplete inversion is more real. For example, if the upper states are 60% populated, a material gain of about 200 cm^{-1} can readily be achieved. Because unipolar lasers can be easily manufactured in the form of dense multicascade structures, such a gain proves to be sufficient for obtaining a mode gain of 20 – 50 cm^{-1}, which is sufficient in turn for lasing.

If the active medium is formed by packets containing three planes each with the quantum-dot density of 10^{11} cm^{-2} and the relaxation time of the upper working level is 10 ps, the relaxation component of the threshold current estimated as 3 kA/cm^2 will be quite acceptable. If the device design ensures the exclusion of various leakage currents, this value will correspond to the lasing threshold.

So long as the distance between the working levels is much greater than the thermal energy, the threshold current will weakly depend on the temperature. For this reason, for wavelengths shorter than 5 μm the lasing threshold will be almost the same at low temperatures and at room temperature (the temperature dependence of the lasing threshold will be determined mainly by the temperature enhancement of absorption by free carriers). It is obvious that to optimise the quantum-dot structure in more detail, a more detailed knowledge of parameters of the medium and processes governing the operating regime is required.

8. Discussion and conclusions

The above analysis demonstrated the possibility of application of quantum-dot structures in unipolar optoelectronic devices such as photodetectors and lasers. Taking into account the use possibility of using wide-band-gap nitride semiconductors, the spectral range of these devices will cover the visible and mid-IR range. We considered the structures in which vertical intracentre optical transitions were used. This operating mechanism suggests that spectral parameters are stable and the output emission can be tuned in a narrower range than in unipolar devices based on diagonal transitions. It seems that threshold parameters can be improved by reducing the spectral bandwidth caused by the scatter in the quantum-dot sizes. In addition, the structure should be optimised in detail to increase the pumping efficiency (spurious currents through the structure should be eliminated) and the mode gain (maximum optical confinement factor), and to reduce reabsorption by free carriers and defects.

Quantum dots offer the following advantages.

(1) Because the energy spectrum of a quantum dot is discrete, thermal broadening of the population distribution does not play a significant role. For this reason, the thermal leveling of population, which causes an increase with temperature in the threshold current in semiconductors is excluded; however, the advantages of injection pumping in semiconductors are retained (low voltage and high efficiency). The laser becomes less sensitive to the ambient temperature, its own overheating, and other temperature variations than other semiconductor lasers.

(2) For the same reason, i.e., because its energy spectrum is discrete, the quantum-dot laser is insensitive to the nonparabolicity of the dispersion of carriers in semiconductors. In other words, the nonparabolicity is no longer a factor of the spectral broadening.

(3) It appears that the nonradiative relaxation of the excited state of a quantum dot proceeds more slowly than in the 2-D electron gas (excluding the resonance relaxation involving optical phonons). For this reason, the quantum-dot unipolar laser should have a lower threshold than the 2-D quantum-well laser under the same conditions. The theoretical analysis [17] showed that the advantage of the

quantum-dot laser in the excited-state relaxation rate could amount to a few orders of magnitude.

(4) The quantum-dot structures offer new principal possibilities for controlling characteristics of emitting objects — 'quasi-atoms'. This concerns the spectral parameters and the directionality and polarisation of emission. One can control the selection rules for the radiative transitions by specifying correctly a profile and geometry of the 3-D potential well. Although at present such a new degree of freedom represents a challenge to modern nanotechnology, the quantum-dot devices already exist which have advantages over the 2-D quantum-well devices related to the selection rules. These are photodetectors for normally incident radiation. Because of the specific selection rules, modern 2-D QWIPs are insensitive to such radiation, whereas quantum-dot structures can detect the normally incident radiation.

We derived the universal (not containing the wavelength) expression (9) for the absorption cross section for intracentre transitions in quantum dots with a parabolic potential well. This expression can be used in the design of unipolar devices operating at various wavelengths in the IR and visible ranges. It is obvious that unipolar quantum-dot optoelectronic devices offer a new approach to the solution of many practical problems (the sensitive detection in the IR region, generation of coherent radiation at various wavelengths in a broad spectral range, optical data processing, and ultra-high-speed optical modulation and switching).

Acknowledgements. The author thanks K Malloy (University of New Mexico) for useful discussions and G A Smolyakov (University of New Mexico) for his help in calculations.

Appendix 1.

The wave functions of the harmonic oscillator

The wave functions of the ground ($1s$) and the first excited ($1p$) states are expressed as products of the radial and angular wave functions:

$$\psi_{00} = A_{00} \exp\left(-\frac{r^2}{2a^2}\right) , \tag{A1.1}$$

$$\psi_{01} = A_{01} r \exp\left(\frac{-r^2}{2a^2}\right) \cos\theta , \tag{A1.2}$$

where r is the radial displacement of a particle from the centre; $a = (\hbar/m^*\omega^2)^{1/2}$ is the characteristic size of the potential well; A_{00} and A_{01} are normalized coefficients; m^* is a mass of the particle; and ω is the angular frequency of the oscillator of the corresponding transition. In the 1-D oscillator, the radius r should be replaced by the coordinate x, and the angular function $\cos\theta$ should be replaced by unity. The normalisation equation

$$\int_{-\infty}^{\infty} \psi^2 \mathrm{d}x = 1 , \tag{A1.3}$$

yields the expressions $A_{00} = \pi^{-1/4}a^{-1/2}$ and $A_{01} = 2^{1/2}\pi^{-1/4} \times a^{-3/2}$. Similarly, for the 2-D oscillator, we have the normalisation equation

$$\int_0^{2\pi}\int_0^{\infty} \psi^2 r \mathrm{d}r\mathrm{d}\theta = 1 , \tag{A1.4}$$

which gives $A_{00} = \pi^{-1/2}a^{-1}$ and $A_{01} = \sqrt{2}\pi^{-1/2}a^{-2}$. For the 3-D oscillator, we have

$$\int_0^{2\pi}\int_0^{\pi}\int_0^{\infty} \psi^2 r^2 \sin\theta \mathrm{d}r\mathrm{d}\theta\mathrm{d}\varphi = 1 , \tag{A1.5}$$

and

$$A_{00} = \pi^{-3/4}a^{-3/2} , \quad A_{01} = \sqrt{2}\,\pi^{-3/4}a^{-5/2} .$$

Appendix 2

Matrix element of the electric dipole moment for the $1s - 1p$ transition

The operator of interaction of linearly polarised light (the polarisation is described by the unit vector ***e*** directed along the electric field of the wave) with the electric dipole ***d*** of the harmonic oscillator is a projection of the dipole moment on the direction of the electric vector of the wave. The matrix element of this dipole moment for the $1s - 1p$ transition is

$$\boldsymbol{ed} = q\langle 01|\boldsymbol{er}|00\rangle, \tag{A2.1}$$

where q is the elementary charge. The dipole transition is allowed because the angular quantum number l changes by unity, whereas the radial (n) and magnetic (m) quantum numbers do not change. Calculations gave the following results.

For the 1-D oscillator, the directions of ***e*** and ***d*** were assumed coincident, and the matrix element is

$$M_{1D} = q\int_{-\infty}^{\infty} \psi_{01} x \psi_{00} \mathrm{d}x$$

$$= qA_{00}A_{01}\int_{-\infty}^{\infty} x \exp(-x^2/a^2)\mathrm{d}x = qa/2^{1/2} . \tag{A2.2}$$

This agrees with the results in Ref. [11],

$$\langle j-1|x|j\rangle = (j/2)^{1/2}a , \tag{A2.3}$$

where $j = 2n + l$ is the principal quantum number in the initial state. For $j = 1$, expressions (A2.2) and (A2.3) give the same result. One can see that the matrix element increases proportionally to $j^{1/2}$, so that the transitions between neighboring excited levels will have a higher probability (proportionally to the number of j of the lower working level) than the transition from the ground state. In the general case, the matrix element depends on the angle β between ***e*** and ***d*** as $\cos\beta$. For the 2-D oscillator, we have

$$M_{2D} = q\int_0^{2\pi}\int_0^{\infty} \psi_{01} r\cos\theta\psi_{00} r\mathrm{d}r\mathrm{d}\theta = qa/2^{1/2} , \tag{A2.4}$$

and for a 3-D oscillator we have

$$M_{3D} = q\int_0^{2\pi}\int_0^{\pi}\int_0^{\infty} \psi_{01} r\cos\theta\psi_{00} r^2\mathrm{d}r\sin\theta\mathrm{d}\theta\mathrm{d}\varphi$$

$$= qA_{00}A_{01}\int_0^{2\pi}\int_0^{\pi}\int_0^{\infty} r^4 \exp(-r^2/a^2)\mathrm{d}r(\cos\theta)^2\sin\theta\mathrm{d}\theta\mathrm{d}\varphi$$

$$= \frac{1}{\sqrt{2}}qa . \tag{A2.5}$$

One can see that the form of the matrix element is the same for harmonic oscillators of different dimensionalities.

References

1. Faist J, Capasso F, Sivco D L, Sirtori C, Hutchinson A L, Cho A Y Science **264** 553 (1994)
2. Levine B F J. Appl. Phys. **74** R1 (1993)
3. Choi K K The Physics of Quantum Well Infrared Photodetectors (New York: World Scientific, 1997)
4. Ruzhii V Semicond. Sci. Technol. **11** 759 (1996)
5. Singh J IEEE Photon. Technol. Lett **8** 488 (1996)
6. Wingreen N S, Stafford C A *IEEE J. Quantum Electron*. **33** 1170 (1997)
7. Vorobjev L E, Firsov D A, Shalygin V A, Tulupenko V N, Shernyakov Yu M, Egorov A Yu, Zhukov A E, Kovsh A R, Kop'ev P S, Kochnev I V, Ledentsov N N, Maximov M V, Ustinov V M, Alferov Zh I Digest IEEE XVI Intern Semicond Laser Conf. (Nara, Japan, 1998) p. 185
8. Tarucha S MRS Bull 6 2 49 (1998)
9. Osinski M, Eliseev P G, Uppal P, Ritter K J II ARL Annual Symposium (College Park, MD, 1998)
10. Belenov E M, Eliseev P G, Oraevskiĭ A N, Romanenko V I, Sobolev A G, Uskov A V Kvantovaya Electron. (Moscow) **15** 1595 (1988) [Sov. J. Quantum Electron. **18** 995 (1988)]
11. Davydov A C Quantum Mechanics (Moscow: Nauka, 1973) pp 163 – 210, 450
12. Faist J, Capasso F, Sirtori C, Sivco D L, Hutchinson A L, Chu S N G, Cho A Y Appl. Phys. Lett. **63** 1354 (1993)
13. West L C, Eglash S J Appl. Phys. Lett. **46** 1156 (1985)
14. Yariv A An Introduction to the Theory and Applications of Quantum Mechanics (New York: J Wiley & Sons, 1982)
15. Pan D, Zeng Y P, Li J M, Zhang C H, Kong M Y, Wang H M, Wang C Y, Wu J J. Cryst. Growth **175/176** 760 (1997)
16. Savage S, Boucaud P, Julien F H, Gerard J-M, Marzin J-Y J. Appl. Phys. **82** 3396 (1997)
17. Benisty H Phys. Rev. B **51** 13281 (1995)